

## PAMELA measurements of the boron and carbon spectra

This content has been downloaded from IOPscience. Please scroll down to see the full text.

2015 J. Phys.: Conf. Ser. 632 012017

(<http://iopscience.iop.org/1742-6596/632/1/012017>)

View [the table of contents for this issue](#), or go to the [journal homepage](#) for more

Download details:

IP Address: 2.225.155.119

This content was downloaded on 02/11/2015 at 13:07

Please note that [terms and conditions apply](#).

## PAMELA measurements of the boron and carbon spectra

N Mori<sup>1,2</sup>, O Adriani<sup>1,2</sup>, G C Barbarino<sup>3,4</sup>, G A Bazilevskaya<sup>5</sup>, R Bellotti<sup>6,7</sup>, M Boezio<sup>8</sup>, E A Bogomolov<sup>9</sup>, M Bongi<sup>1,2</sup>, V Bonvicini<sup>8</sup>, S Bottai<sup>2</sup>, A Bruno<sup>6,7</sup>, F Cafagna<sup>7</sup>, D Campana<sup>4</sup>, R Carbone<sup>8</sup>, P Carlson<sup>13</sup>, M Casolino<sup>10,14</sup>, G Castellini<sup>15</sup>, C De Donato<sup>10,11</sup>, C De Santis<sup>10,11</sup>, N De Simone<sup>10</sup>, V Di Felice<sup>10,18</sup>, V Formato<sup>8,16</sup>, A M Galper<sup>12</sup>, A V Karelin<sup>12</sup>, S V Koldashov<sup>12</sup>, S Koldobskiy<sup>12</sup>, S Y Krutkov<sup>9</sup>, A N Kvashnin<sup>5</sup>, A Leonov<sup>12</sup>, V Malakhov<sup>12</sup>, L Marcelli<sup>10,11</sup>, M Martucci<sup>11,19</sup>, A G Mayorov<sup>12</sup>, W Menn<sup>17</sup>, M Mergé<sup>10,11</sup>, V V Mikhailov<sup>12</sup>, E Mocchiutti<sup>8</sup>, A Monaco<sup>6,7</sup>, R Munini<sup>8,16</sup>, G Osteria<sup>4</sup>, F Palma<sup>10,11</sup>, B Panico<sup>4</sup>, P Papini<sup>2</sup>, M Pearce<sup>13</sup>, P Picozza<sup>10,11</sup>, M Ricci<sup>19</sup>, S B Ricciarini<sup>2,15</sup>, R Sarkar<sup>20,21</sup>, V Scotti<sup>3,4</sup>, M Simon<sup>17</sup>, R Sparvoli<sup>10,11</sup>, P Spillantini<sup>1,2</sup>, Y I Stozhkov<sup>5</sup>, A Vacchi<sup>8</sup>, E Vannuccini<sup>2</sup>, G I Vasilyev<sup>9</sup>, S A Voronov<sup>12</sup>, Y T Yurkin<sup>12</sup>, G Zampa<sup>8</sup> and N Zampa<sup>8</sup>

<sup>1</sup>University of Florence, Department of Physics and Astronomy, I-50019 Sesto Fiorentino, Florence, Italy

<sup>2</sup>INFN, Sezione di Florence, I-50019 Sesto Fiorentino, Florence, Italy

<sup>3</sup>University of Naples "Federico II", Department of Physics, I-80126 Naples, Italy

<sup>4</sup>INFN, Sezione di Naples, I-80126 Naples, Italy

<sup>5</sup>Lebedev Physical Institute, RU-119991, Moscow, Russia

<sup>6</sup>University of Bari, Department of Physics, I-70126 Bari, Italy

<sup>7</sup>INFN, Sezione di Bari, I-70126 Bari, Italy

<sup>8</sup>INFN, Sezione di Trieste, I-34149 Trieste, Italy

<sup>9</sup>Ioffe Physical Technical Institute, RU-194021 St Petersburg, Russia

<sup>10</sup>INFN, Sezione di Rome "Tor Vergata", I-00133 Rome, Italy

<sup>11</sup>University of Rome "Tor Vergata", Department of Physics, I-00133 Rome, Italy

<sup>12</sup>National Research Nuclear University MEPhI, RU-115409 Moscow

<sup>13</sup>KTH, Department of Physics, and the Oskar Klein Centre for Cosmoparticle Physics, AlbaNova University Centre, SE-10691 Stockholm, Sweden

<sup>14</sup>RIKEN, Advanced Science Institute, Wako-shi, Saitama, Japan

<sup>15</sup>IFAC, I-50019 Sesto Fiorentino, Florence, Italy

<sup>16</sup>University of Trieste, Department of Physics, I-34147 Trieste, Italy

<sup>17</sup>Universität Siegen, Department of Physics, D-57068 Siegen, Germany

<sup>18</sup>Agenzia Spaziale Italiana (ASI) Science Data Center, Via del Politecnico snc I-00133 Rome, Italy

<sup>19</sup>INFN, Laboratori Nazionali di Frascati, Via Enrico Fermi 40, I-00044 Frascati, Italy

<sup>20</sup>Indian Centre for Space Physics, 43, Chalanika, Garia Station Road, Kolkata 700 084, West Bengal, India

<sup>21</sup>Previously at INFN, Sezione di Trieste, I-34149 Trieste, Italy

E-mail: mori@fi.infn.it



**Abstract.** The satellite-borne PAMELA experiment is aimed at precision measurements of the charged light component of the cosmic-ray spectrum, with a particular focus on antimatter. It consists of a magnetic spectrometer, a time-of-flight system, an electromagnetic calorimeter with a tail catcher scintillating layer, an anticoincidence system and a neutron detector. PAMELA has measured the absolute fluxes of boron and carbon and the B/C ratio, which plays a central role in galactic propagation studies in order to derive the injection spectra at sources from measurements at Earth. In this paper, the data analysis techniques and the final results are presented.

## 1. Introduction

During the propagation in the interstellar medium (ISM) from the acceleration sites to Earth, galactic cosmic rays undergo various physical processes which shape the injection spectra and chemical compositions down to the measured ones at Earth. Knowledge of these processes is required in order to interpret the measurements in terms of the parameters of the acceleration sources, or to estimate the backgrounds when searching for new and possibly faint contributions to the spectra.

Currently, there is still uncertainty in determining which are the most relevant physical processes [1]. The usual modelization of propagation is given in terms of a diffusive transport equation with source terms [2]. The equation accounts for diffusion, convection due to the interaction with the galactic wind, re-acceleration, spallation and radioactive decay. Direct measurements of astrophysical quantities (e.g. the hydrogen density obtained from 21-cm surveys) and fits of the distributions obtained from numerical propagation models to cosmic-ray measurements provide the parameters of the equation.

The spectra of particles which are produced exclusively by interactions of primary particles with ISM provide good constraints to propagation parameters. In particular, boron nuclei in cosmic rays are produced mainly by spallation of carbon with contributions from other elements. The boron-to-carbon ratio (B/C) has been measured by many experiments [3] and extensively studied in order to tune and benchmark propagation models (see e.g. [4] and references therein).

The PAMELA experiment [5] has recently measured the spectra of boron and carbon as well as the B/C ratio in the kinetic energy range 0.44 - 129 GeV/n [6]. In this paper the data analysis techniques and the final results for the data acquired during the period July 2006 - March 2008 are presented. Section 2 describes the detector while the data analysis procedures are detailed in section 3. The results are presented in section 4.

## 2. The PAMELA detector

The PAMELA main detector is a magnetic spectrometer made by tracking system placed inside the magnetic field generated by a permanent magnet. The tracking system consists of six double-sided silicon microstrip tracking layers; the readout pitches for the X (bending) and Y views are 51  $\mu\text{m}$  and 66.5  $\mu\text{m}$ , respectively. The intensity of the magnetic field at the center of the magnetic cavity is 0.46 T. The main aim of the tracking system is to measure the magnetic rigidity  $\rho = pc/(Ze)$  of the impinging primary particle, from whose sign antimatter can be discerned from matter. The instrument trigger is provided by the Time-Of-Flight (TOF) system. It is composed by six layers of plastic scintillating pads arranged in three X-Y layers, two of them (named S1 and S2) above the tracking system and the third (S3) below it. The TOF also measures the particle velocity with a resolution of 250 ps for  $|Z|=1$  particles and 70 ps for carbon [7] and the particle electric charge via multiple ionization measurements. The tracking system and the TOF are shielded by an anticoincidence system made by plastic scintillators, which allows interacting events producing secondary particles to be rejected during the offline analysis. A silicon-tungsten sampling electromagnetic calorimeter is placed below S3. It is

made by 22 modules, each composed by two single-sided silicon strip detectors encompassing a tungsten converter layer. The readout pitch of the strips is 2.44 mm and the total depth is  $16.3 X_0$ . The calorimeter provides a direct measurement of the energy of electrons and positrons. Due to its lateral segmentation a lepton/hadron rejection power of about  $10^5$  by means of topological shower analysis can be achieved. The rejection power is further improved by a tail-catcher scintillator and a neutron detector, both placed below the calorimeter.

For a detailed description of the PAMELA instrument and its performance see [5].

### 3. Data analysis

The PAMELA design and data analysis procedures have been optimized for  $|Z| \sim 1$  particles, given its main focus on antimatter measurements (mainly positrons and antiprotons). In particular, an effect of this optimization is that the front-end readout electronics of the tracking system saturates when a high- $Z$  particle like a boron or carbon nuclei crosses a silicon layer of the spectrometer releasing a high quantity of energy via ionization. This saturation produce systematic effects like a displacement of the tracking residuals when processing data with the algorithms conceived for  $|Z| \sim 1$  particles. In order to get rid of these systematic effects, a position finding algorithm optimized for boron and carbon has been developed. This algorithm emulates a digital readout of saturated strip signals, which are then clustered before computing the impact point as the geometric center of the cluster ignoring all non-saturated strips. The spatial resolution obtained with this algorithm is  $14 \mu\text{m}$  on the X (bending) view and  $19 \mu\text{m}$  on the Y view, resulting in a Maximum Detectable Rigidity (MDR) of about 250 GV.

Before applying the tracking algorithm, clusters of strips with a total energy release less than 5 MIP have been discarded (an energy release of 1 MIP is defined as the energy released by a  $|Z|=1$  minimum-ionizing particle). This selection removes the clusters produced by backscattered particles coming from the calorimeter or by delta rays, resulting in a higher tracking efficiency.

Events have been selected by requiring a single, well-fitted track with at least 4 associated hits on the X view and 3 on the Y view, in order to have a reliable measurement of the rigidity of the incoming particle. The track is required to lie inside the magnetic cavity of the spectrometer and to stay at least 1.5 mm away from the walls of the magnet, to reject particles crossing the magnet itself. This fiducial volume corresponds to a geometric acceptance of  $19.9 \text{ cm}^2 \text{ sr}$ ; this value has been used for computing the fluxes. Particles have also been requested to be down-going according to the TOF system. Galactic particles have been selected by imposing the requirement that the measured rigidity  $\rho$  exceeds the critical rigidity  $\rho_C$  computed in the Störmer vertical approximation by a factor of 1.3.

Boron and carbon events have been selected by means of their ionization energy releases in the TOF system, which grows as  $Z^2$  at relativistic energies. Fig. 1 shows the mean (indicated with  $\langle S2 \rangle$ ) of the energy releases detected by each of the two layers of scintillating pads constituting S2 as a function of the rigidity  $\rho$ . The figure also shows the selection criteria used to identify boron and carbon based on these measurement. Similar criteria are built also for S12 (the lower of the two layers constituting S1) and  $\langle S3 \rangle$  (mean of ionization releases on the two layers constituting S3). Particles have been tagged as boron or carbon if they satisfy all the three charge selection criteria on S12,  $\langle S2 \rangle$  and  $\langle S3 \rangle$ .

The efficiencies of the selection cuts described above have been measured directly from flight data. Tracking efficiency has been evaluated on a sample of non-interacting boron and carbon events selected with the TOF system whose track fitted in the calorimeter and extrapolated back to the top of payload lies entirely inside the fiducial acceptance. The energy dependence of the efficiency has been obtained at low energies by means of the velocity  $\beta$  measured by the TOF. However, at high energies there is no way to evaluate the energy dependence from flight data. Moreover, requiring a fitted track in the calorimeter makes the selected sample non-isotropic due to the additional request that the primary exits from the bottom side of the calorimeter itself:

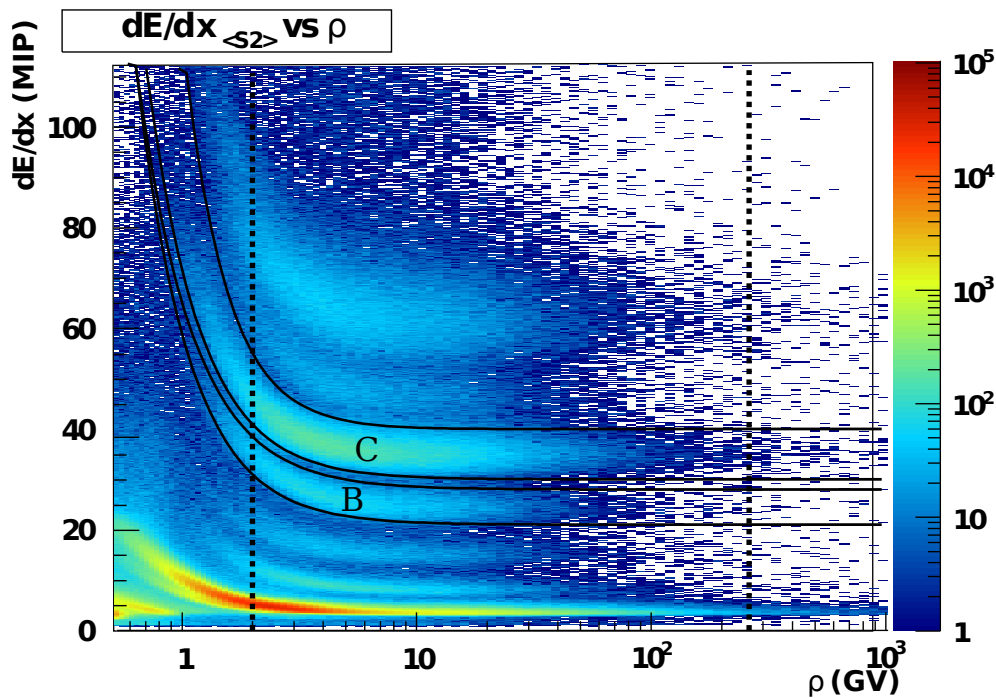


**Figure 1.** Mean ionization release and charge selection bands for  $\langle S2 \rangle$ . The vertical dashed lines indicate the limits in rigidity of this analysis.

this ensures a good lever arm for the fit but rejects those inclined tracks which lie inside the acceptance of the instrument without crossing the last layer of the calorimeter. In order to cope with these two issues, a rigidity-dependent efficiency has been evaluated also on an isotropic sample obtained from Monte Carlo simulations. This efficiency has been subsequently divided by a Monte Carlo efficiency obtained with the same procedure used for flight data, resulting in a rigidity-dependent correction factor for the experimental efficiency. This factor is almost constant at a value of 0.97.

The efficiency of charge selection has been measured on a sample of pure boron or carbon selected by means of ionization measurements in S11 (the upper layer of S1) and in the first silicon layer of the calorimeter. These two detectors encompass the whole instrument from top to bottom, thus this selection rejects those events where the primary fragments in the apparatus due to nuclear interactions. The resulting efficiency peaks at about 75% at 3 GV for both species and then decreases with increasing energy, reaching an almost constant value of about 50% for boron and 60% for carbon above 30 GV. The presence of a possible residual contamination in the sample used to measure the efficiency has been investigated by measuring the variation of the selection efficiency of S12 when also  $\langle S2 \rangle$  and  $\langle S3 \rangle$  are used to pre-select the sample for efficiency measurement. No statistically significant variation have been observed, also when repeating the same procedure for the efficiencies of  $\langle S2 \rangle$  and  $\langle S3 \rangle$ .

Monte Carlo simulations have been used to compute correction factors for various instrumental effects that cannot be investigated with flight data. Nuclear interactions in the aluminum dome on top of the instrument which destroy primaries or sweep them away from the acceptance of the detector have been investigated with a Fluka simulation [8]. The correction amounts to 14% for boron and 15% for carbon above 10 GV, where the dominant contribution is from inelastic scattering which destroys the primary. The value of the correction factor increases for both species at low energies where elastic scattering can significantly modify the trajectory of the primary and energy losses in the apparatus can significantly lower the energy of the particle,

which is then swept away by the magnetic field of the instrument. Fluka simulations have been used also to quantify the production of secondaries by fragmentation of heavier species in the dome. This effect is negligible for carbon, while for boron it results in a correction factor of about 5% at some GV rising to about 20% at 200 GV, given mainly by spallation of carbon. Folding effects due to the finite rigidity resolution of the magnetic spectrometer and energy losses in the instrument (which can significantly affect the measured rigidity of particles at very low energies) have been corrected by means of a Bayesian unfolding procedure [9], using a Geant4 simulation [10] in order to obtain the smearing matrix. Since the selection of galactic particles has been done before correcting for slow down effects, some events may have been incorrectly rejected due to their rigidity being reduced by energy losses in the apparatus; a correction factor for this effect has been computed with Geant4 simulations. It amounts to 0.97 at 2 GV and it rises with energy reaching the value 1 (i.e. no correction) at 3 GV and above.

Since the events are binned according to their measured rigidity it is necessary to take into account the isotopic composition of boron when computing the boron flux as a function of kinetic energy per nucleon. Both  $^{10}\text{B}$  and  $^{11}\text{B}$  are present in cosmic rays, and their relative abundance is a poorly-known parameter. At relativistic energies no direct measurement is available. Estimations can be made using galactic propagation models, and the current consensus value for the  $^{10}\text{B}$  fraction (defined as  $^{10}\text{B}/(^{10}\text{B}+^{11}\text{B})$ ) is  $0.35\pm 0.15$  and has a weak dependence on energy. But since different isotopes of the same energy have different rigidities, then the fraction is not constant when it is expressed as a function of rigidity. The procedure used to compute the rigidity-dependent  $^{10}\text{B}$  fraction starting from the energy-independent  $^{10}\text{B}$  fraction and the consequent boron event count as a function of kinetic energy per nucleon is described in details in appendix A of [6].

An accurate study of the systematic uncertainties of the measurement has been done considering various effects: the finite sizes of the samples used to measure the selection efficiencies and to compute correction factors, the effect of the residual contamination in the samples used to measure the charge selection efficiencies and the fluxes, the residual misalignment of the spectrometer, the requirement of fiducial containment, the disagreement between tracking efficiencies computed with flight data and with Monte Carlo data, the uncertainty on the unfolding procedure (assessed with a fold/unfold test) and the uncertainty in the isotopic composition of boron. The quadratic sum of all these factors give a total systematic uncertainty of about 6% at low energy for both species, rising to about 7% at high energy for carbon and to 10% for boron.

The live time of the instrument has been obtained from on-board clocks, and has been computed as a function of the cutoff rigidity to account for the different amount of time spent by PAMELA at different latitudes. The live time spent in regions where the cutoff value is above 2 GV is  $1 \times 10^7$  s, increasing up to  $3.14 \times 10^7$  s for regions with cutoff above 20 GV. The associated error is about 0.2% and has been neglected.

#### 4. Results

The boron and carbon fluxes and the boron-over-carbon (B/C) ratio measured by PAMELA as functions of kinetic energy per nucleon are shown in fig. 2.

A quite good agreement with previous measurements can be observed, except at low energy where the effects of solar modulation are significant and must be carefully taken into account when comparing fluxes measured in different solar periods. The fitted spectral indexes above 20 GeV/n are  $3.01\pm 0.13$  for boron and  $2.72\pm 0.06$  for carbon. A very simple fit of PAMELA data based on the GALPROP transport code [11] gives a slope of the diffusion coefficient of  $0.397\pm 0.007$ , thus not allowing to discriminate between Kolmogorov and a Kraichnan diffusion types. However, this figure has been obtained with a specific transport code/model, and may vary when using different codes/models. Tighter constraints on propagation models and

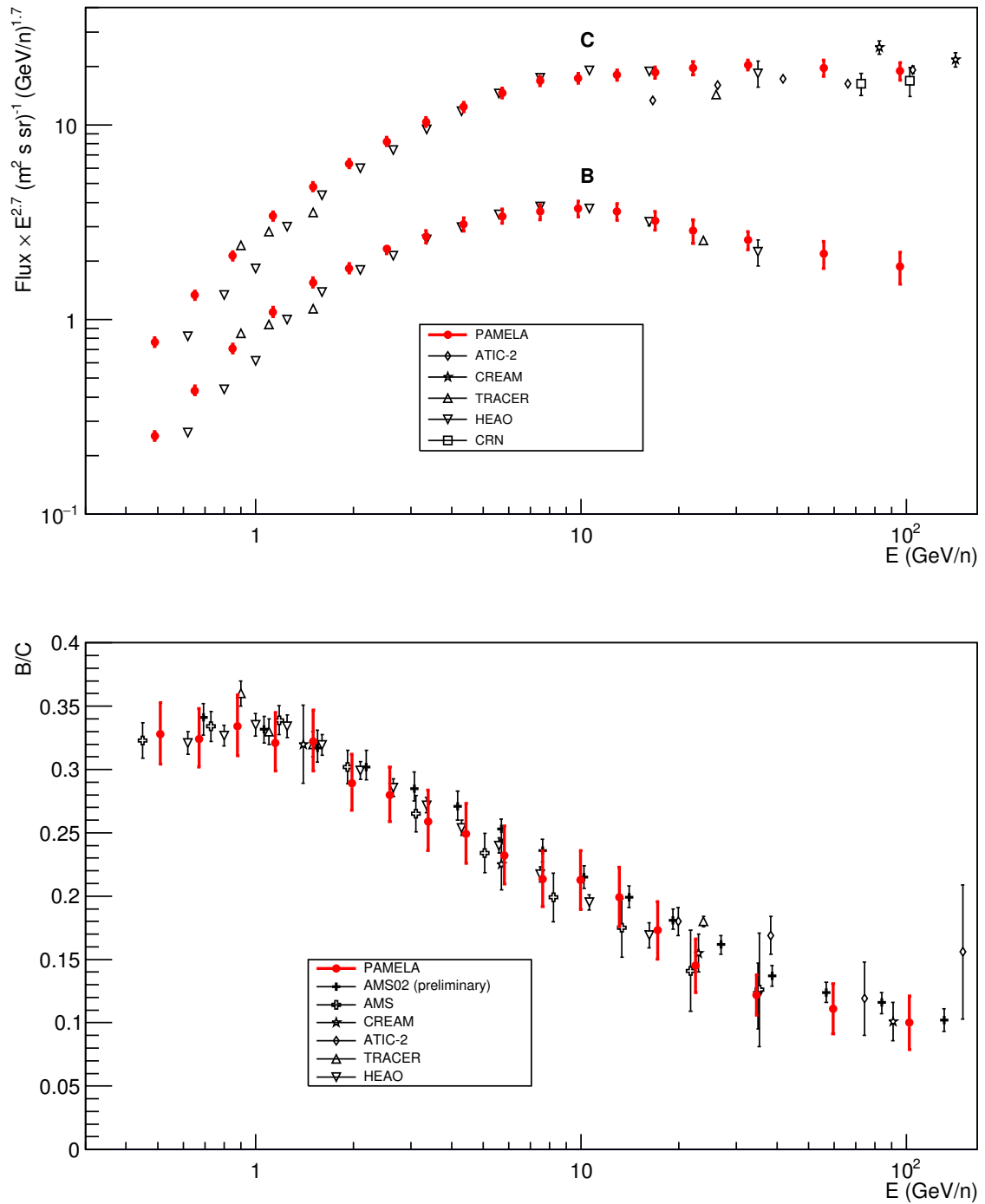


**Figure 2.** Boron and carbon fluxes multiplied by  $E^{2.7}$  (upper panel) and B/C flux ratio (lower panel) as measured by PAMELA, together with results from other experiments [3]. The error bars for PAMELA are the quadratic sum of the statistical and the systematical contributions.

parameters could be obtained including also other quantities like the isotopic ratios of the lightest nuclei (i.e. the  $^2\text{H}/^1\text{H}$  and  $^3\text{He}/^4\text{He}$  ratios [12]) in the fit.

### Acknowledgments

We acknowledge support from The Italian Space Agency (ASI), Deutsches Zentrum für Luft- und Raumfahrt (DLR), The Swedish National Space Board, The Swedish Research Council, The Russian Space Agency (Roscosmos) and The Russian Science Foundation.

### References

- [1] Maurin D, Putze A and Derome L 2010 *Astron. & Astroph.* **516** A67
- [2] Ptuskin V 2012 *Astropart. Phys.* **39-40** 44
- [3] Oliva A *et al* (AMS collaboration) *33rd International Cosmic Ray Conference (ICRC 2013)*  
<http://www.cbpf.br/~icrc2013/proceedings.html>  
Ahn H S, Allison P S, Bagliesi M G *et al* 2008 *Astropart. Phys.* **30** 133  
Obermeier A, Ave M, Boyle P *et al* 2011 *Astroph. Journ.* **742** 14  
Panov D, Sokolskaya N V, Adams J H Jr *et al* 2007 *30th International Cosmic Ray Conference (ICRC 2007)*  
3, ed R Caballero, J C D'Olivo *et al*  
Engelmann J J, Ferrando P, Soutoul A *et al* 1990 *Astron. & Astroph.* **233** 96  
Aguilar M, Alcaraz J, Allaby J *et al* 2010 *Astroph. Journ.* **724** 329  
Swordy S P, Müller D, Meyer P *et al* 1990 *Astroph. Journ.* **349**,625
- [4] Obermeier A, Boyle P, Hörandel J and Müller D 2012 *Astroph. Journ.* **752** 69
- [5] Picozza P, Galper A M, Castellini G *et al* 2007 *Astropart. Phys.* **27** 296
- [6] Adriani A, Barbarino G C, Bazilevskaya G A *et al* 2014 *Astroph. Journ.* **791** 93
- [7] Campana D, Carbone R, De Rosa G *et al* 2009 *Nucl. Inst. and Meth. in Phys. A* **598** 696
- [8] Battistoni G, Muraro S, Sala P R *et al* 2007 *Hadronic Simulation Workshop 2006*, ed M Albrow & R Raja, 31
- [9] D'Agostini G 1995 *Nucl. Inst. and Meth. in Phys. A* **362** 487
- [10] Agostinelli S, Allison J, Amako K *et al* 2003 *Nucl. Inst. and Meth. in Phys. A* **506** 250
- [11] Strong A and Moskalenko I V 1998 *Astroph. Journ.* **509** 212
- [12] Adriani A, Barbarino G C, Bazilevskaya G A *et al* 2013 *Astroph. Journ.* **770** 2